Beginning of the great Mw = 9.0 Tohoku-Oki earthquake

Risheng Chu[1,2], Shengji Wei[1,2], Hiroo Kanamori[1,2], Don V. Helmberger[1,2], and Zhongwen Zhan[1,2]

[1]Seismological Laboratory, California Institute of Technology, Pasadena, CA 91125 [2]Tectonic Observatory, California Institute of Technology, Pasadena, CA 91125

Abstract

Epicenter of large subduction-zone earthquakes is often used as a reference point for finite-fault inversions and back-projection mapping. However, these earthquakes generally lack regional seismic stations in the off-shore direction leading to diverse epicenter estimates. Here we use the differential timing between the water phase reflected from the air-water interface and the depth phase reflected from the water-crust interface to help locate a master earthquake using the well-known ocean bathymetry. After calibrating teleseismic arrays (30° to 90°) at short periods for timing and amplitude with respect to the master event, we are able to study the beginning 4 sec of teleseismic body waves of the great 2011 Tohoku-Oki earthquake, which began with a thrust event (Mw = 4.9) located at 38.19N, 142.68E at a depth of about 21 km.

Introduction

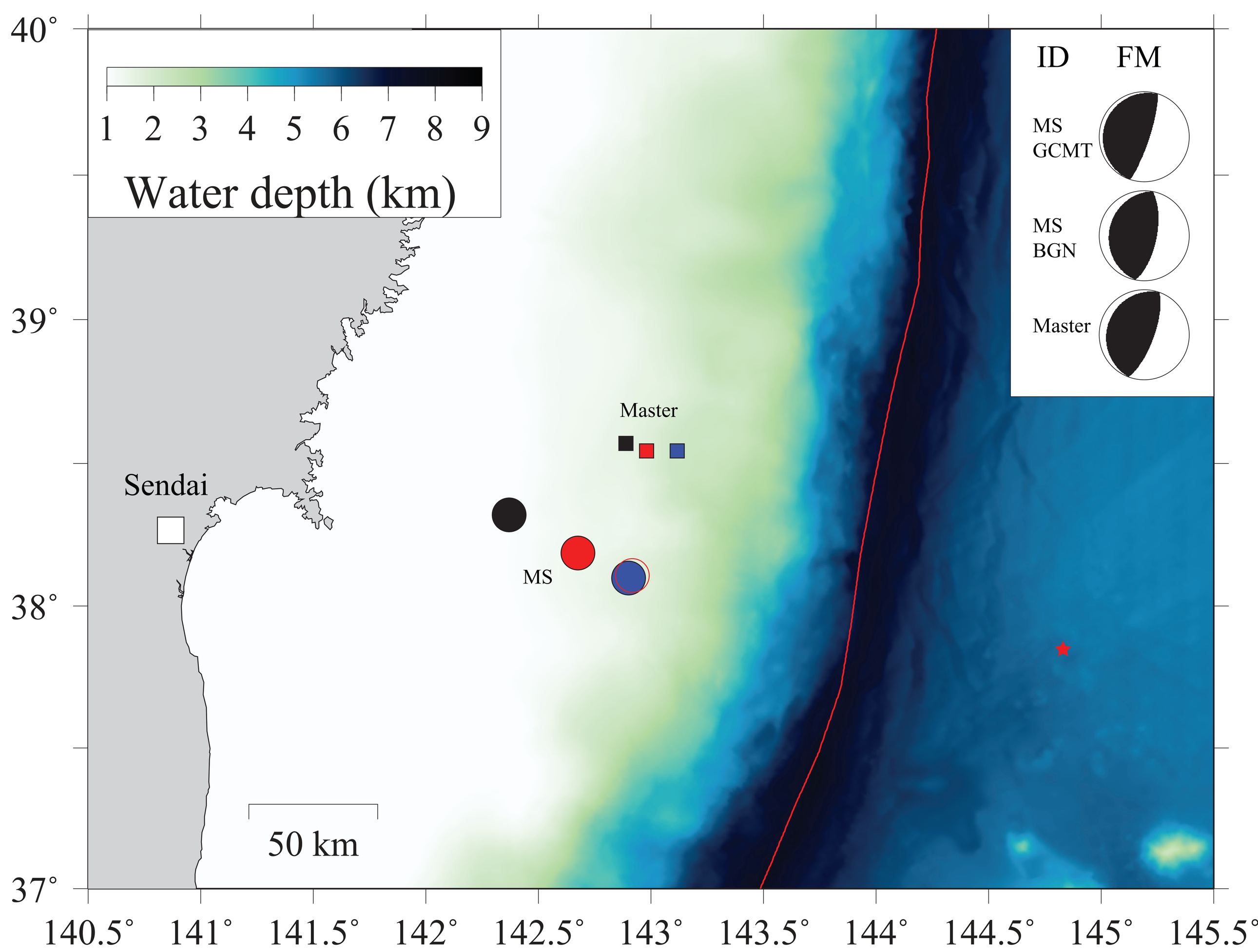

Figure 1. Map of the off-shore epicentral region of the great 2011 Tohoku-Oki earthquake (circles) along with the 2008 master event (squares) and the 2011 outer-rise earthquake (red star). Black and blue symbols denote locations from the NEIC and JMA catalog, respectively. Red open circle represents the epicenter of the 2011 Tohoku-Oki earthquake by Zhao et al. (2011). The red square and circle denote our preferred locations by modeling teleseismic water waves for the master event and mainshock. The 0.5-km bathymetric grid of the sea floor is obtained from the Japan Oceanographic Data Center. The red line denotes the subduction trench (Bird, 2003). The inset displays the focal mechanisms of the mainshock inverted by global CMT, the beginning of the mainshock, and the master earthquake, respectively.

Teleseismic water phases

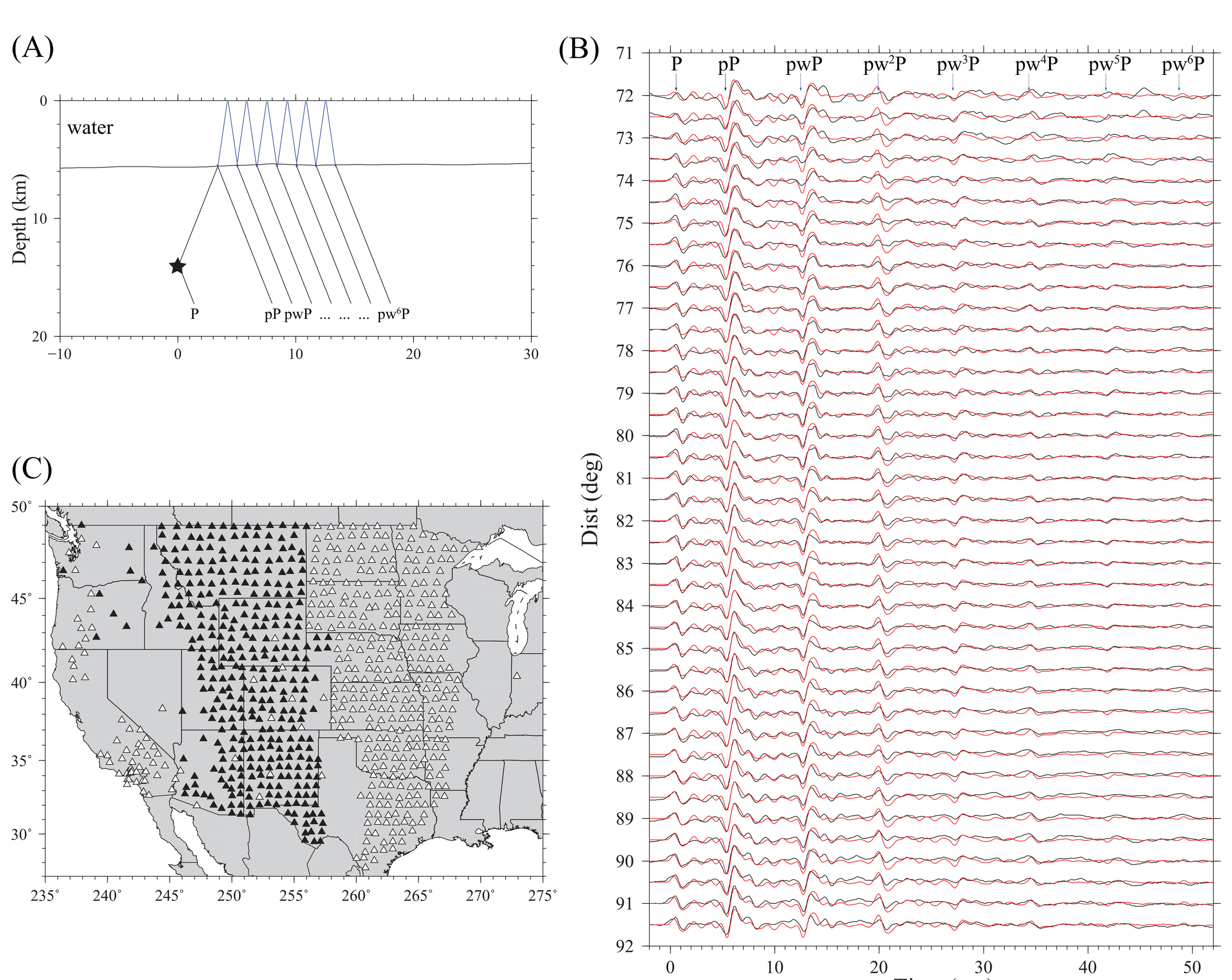

Figure 2. An example of the teleseismic water phases. (A) A sketch of the water geometry and the ray paths of teleseismic water phases. Because of the large velocity contrast of the water surface, an earthquake can generate extra sets of P-wave depth phases, pwP and swP, and their multiple reverberations besides phases reflected from the top of the oceanic crust (Engdahl et al., 1998). (B) A record section of the outer-rise earthquake recorded by USArray stations. 417 seismograms are stacked using a bin size of 0.5°. The depth phase pP and water phases are labeled on the top with black and blue arrows, respectively. Synthetic seismograms are calculated using a velocity model from seismic experiment in the area (Takahashi et al., 2004) and a uniform water depth of 5.5 km. (C) Map of the USArray stations recording the 03/11/2011 outer-rise earthquake (white triangles). Black triangles recorded the 12/04/2008 master earthquake shown in Figure 3.

The 2008 master earthquake

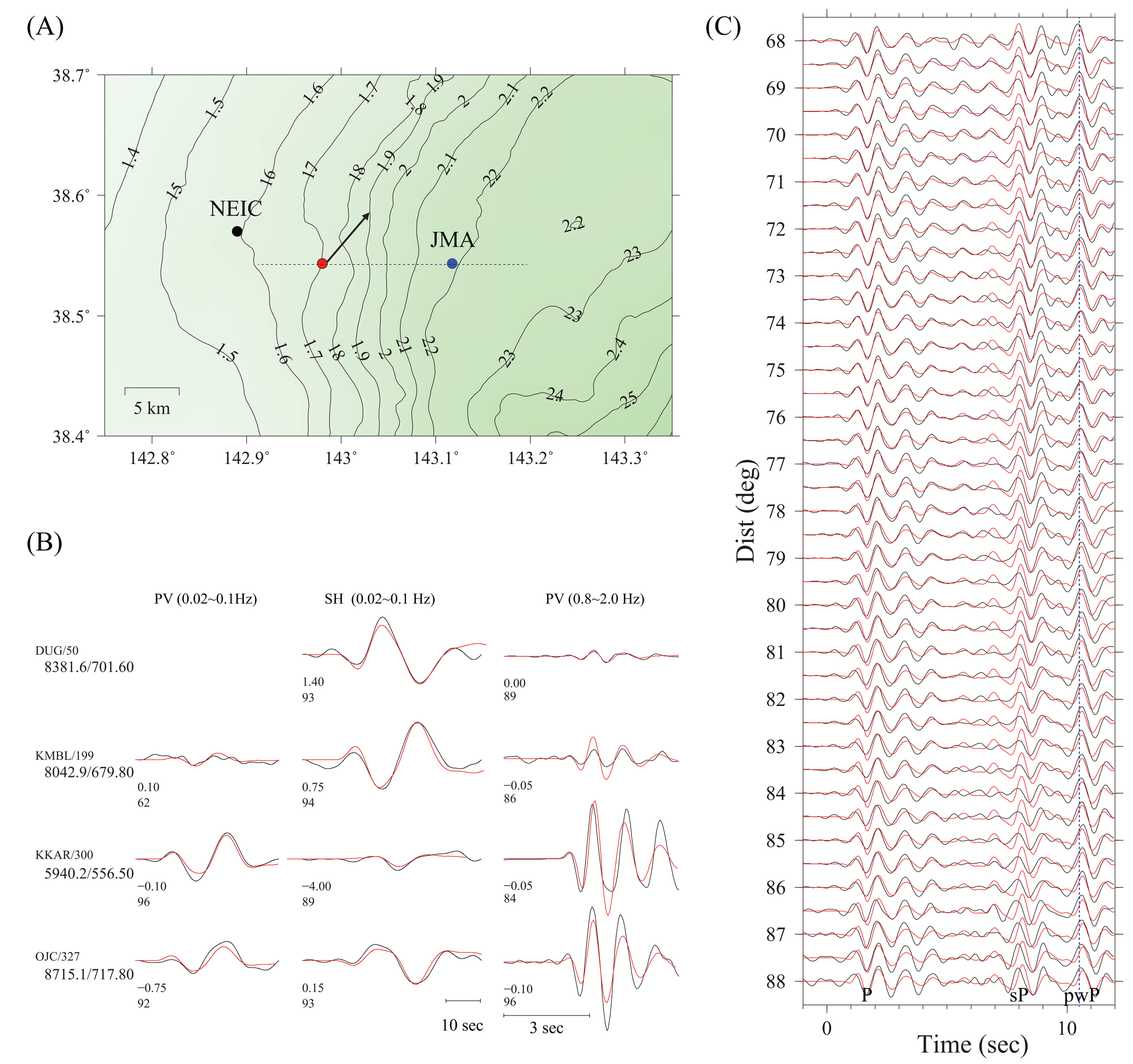

Figure 3. Relocating the 2008 master earthquake using water phases. (A) Locations from NEIC and JMA catalogs are plotted as black and blue dots, respectively. The red dots represent the refined location. The arrows indicate the averaged azimuth of the USArray and the arrowhead represents the reflecting point of pwP at ocean surface. Black contours are water depth with an increase of 0.1 km. (B) Sample of waveform fits in the calibration of master event. We cut each seismogram into P and SH segments and allow a maximum shift of 5.0 sec to find the best fits using the Cut-and-Paste (CAP) method (Zhu and Helmberger, 1996). The number after the station name is the azimuth. Two numbers below station names are the epicentral distance in km and initial picked arrival time (tn). Two numbers below the seismogram are the time shift and cross-correlation coefficient (CCs) after inverting the waveforms. The earthquake has a mechanism with strike/dip/rake of 200°/18°/90° at a depth of 21 km. Representative waveform fits are shown as data (black) and synthetics (red). We repeat the same procedure at a relative higher frequency (0.8-2.0 Hz). Because depth phases are contaminated by complex structure above the earthquake, we only use direct P from 154 stations allowing a maximum shift of 0.5 sec. Most of the waveform fits have CCs larger than 0.80 (Figure S3). Accurate arrival times can be obtained by adding tn and the corresponding time shift from waveform fits. Path calibration for each station can be accurately obtained at this high frequency range. (C) Stacking of the waveforms recorded by USArray at frequency range of 0.8-2.0 Hz is shown as black seismogram with P, pP, and pwP phases labeled. Synthetic seismograms (red) are for the water depth of 1.9 km. We use JMA's latitude (dashed line in A) and a grid search in the EW direction is conducted to find this best location.

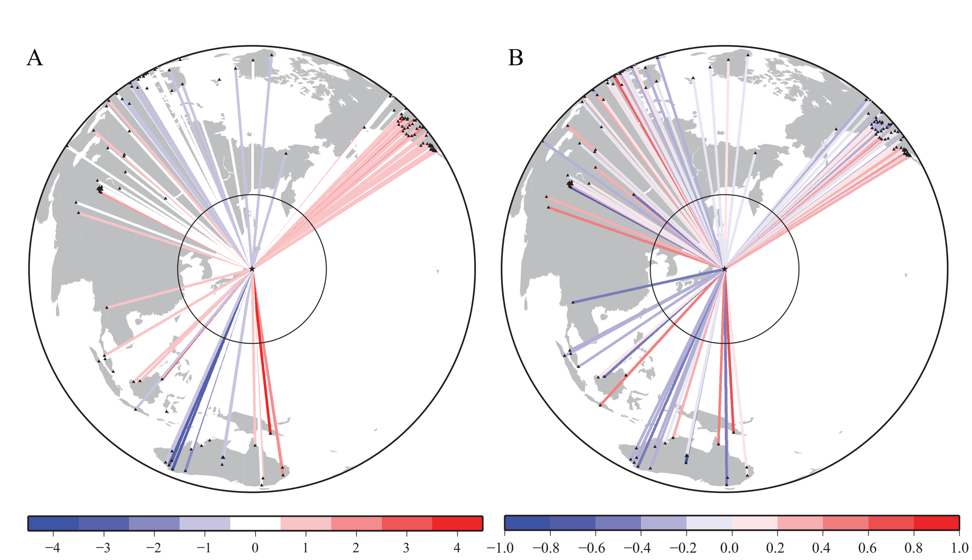

Figure S1. Travel-time delays (A) and AAF (B) for the 2008 master earthquake at teleseismic distances using the refined location. Negative and positive delays mean faster and slower arrivals, respectively. Slow paths generally have amplitude amplified (red color), while fast paths have small amplitude (blue color).

Locating the 2011 Tohoku-Oki earthquake

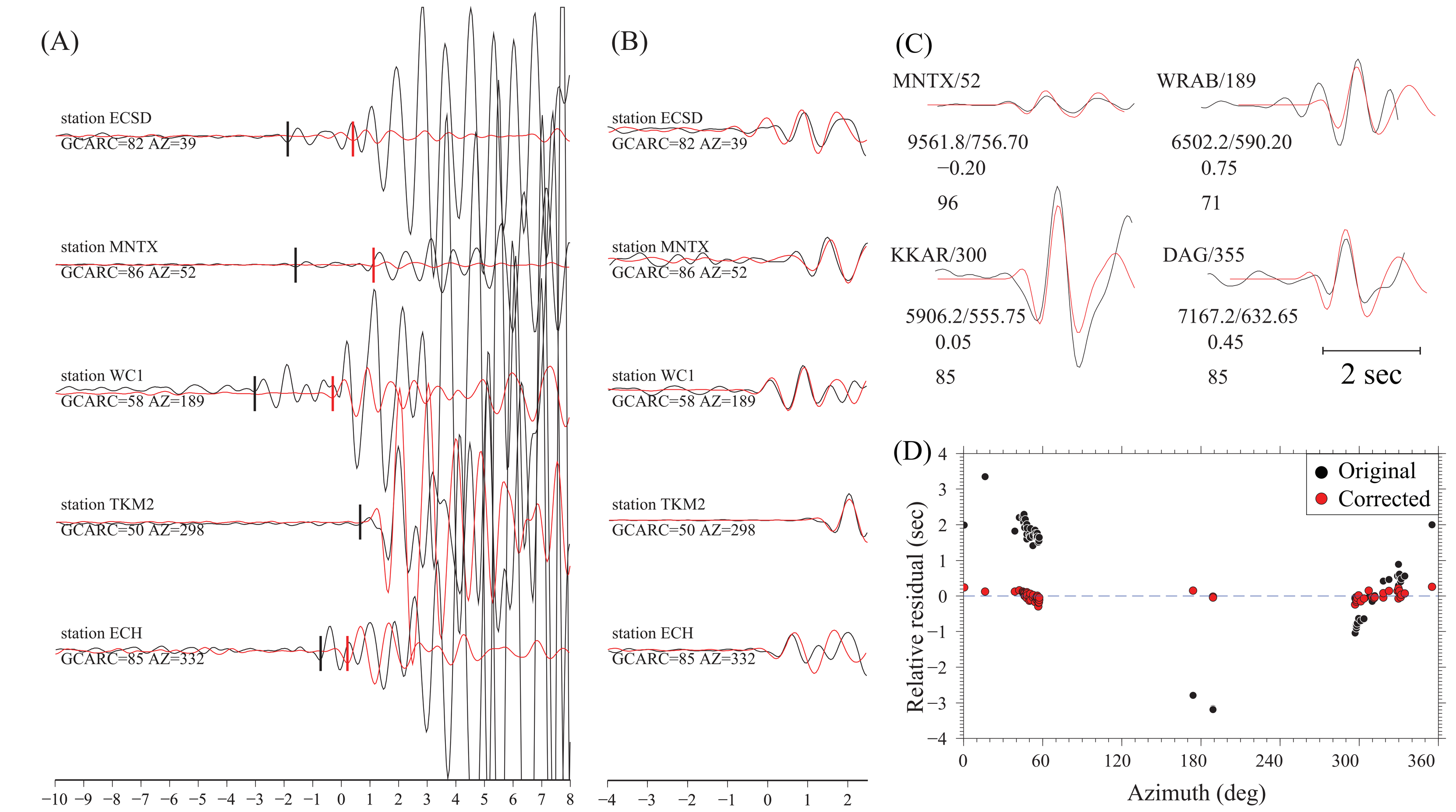

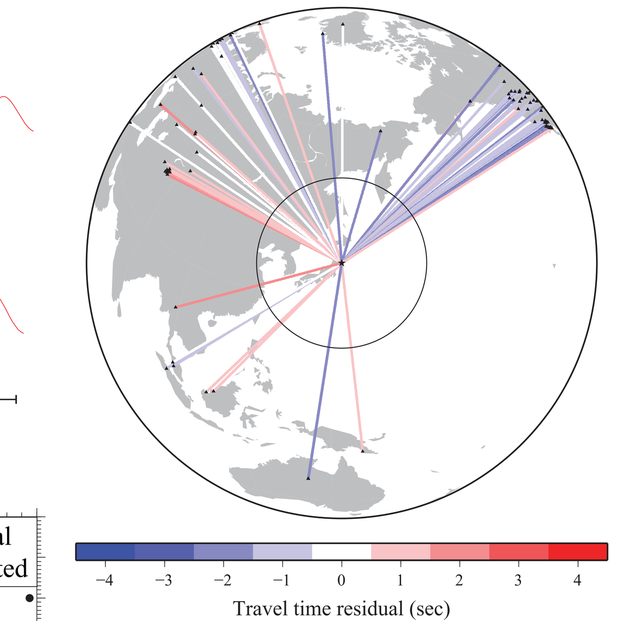

Figure S2. Travel-time delays of the mainshock using NEIC location. Differential travel times between the master earthquake and the mainshock at each station, shown in Figure 4B can be obtained using delays in Figure S1(A). The differential travel times can be used to calculate their relative locations.

Figure 4. Focal mechanism and relocation for the beginning of the main rupture. (A) Comparison of waveforms at 0.8-2.0 Hz for the mainshock (black) and the master earthquake (red) for a sample of 5 teleseismic stations. All seismograms are aligned with IASPEI91 predictions using the refined location for the master event and NEIC location for the mainshock. Since beginning of the mainshock has the magnitude 0.4 smaller than the master event, all black traces are multiplied by 2 for display purpose. Black and red vertical bars denote arrival time of the mainshock and master event, respectively. (B) Comparison of data for the first 2.5 sec from these two earthquakes aligned with IASPEI91 predictions. The seismograms are normalized to the maximum amplitudes. The epicenter of mainshock is the refined location. Waveforms from the master earthquake and the mainshock match very well, which confirms the accuracy of the refined location. (C) The first 4.0 sec of 82 recordings with relatively low noise levels were used in the CAP inversion with 4 examples displayed. Observed data and synthetics are displayed in black and red waveforms, respectively. The number after the name is the azimuth; the lower numbers indicate the distance in km and initial timing in seconds followed by two numbers indicating time shift and the CC. Each seismogram has been corrected by the AAFs from the master event. A maximum shift of 1.0 sec is allowed and the solution with strike/dip/rake at 191°/23°/90° is obtained. (D) Relative travel-time residuals of the mainshock with respect to the master event is shown as black dots. Red dots denote residuals corrected with respect to the new location given as the red star in Figure 1.

Discussion

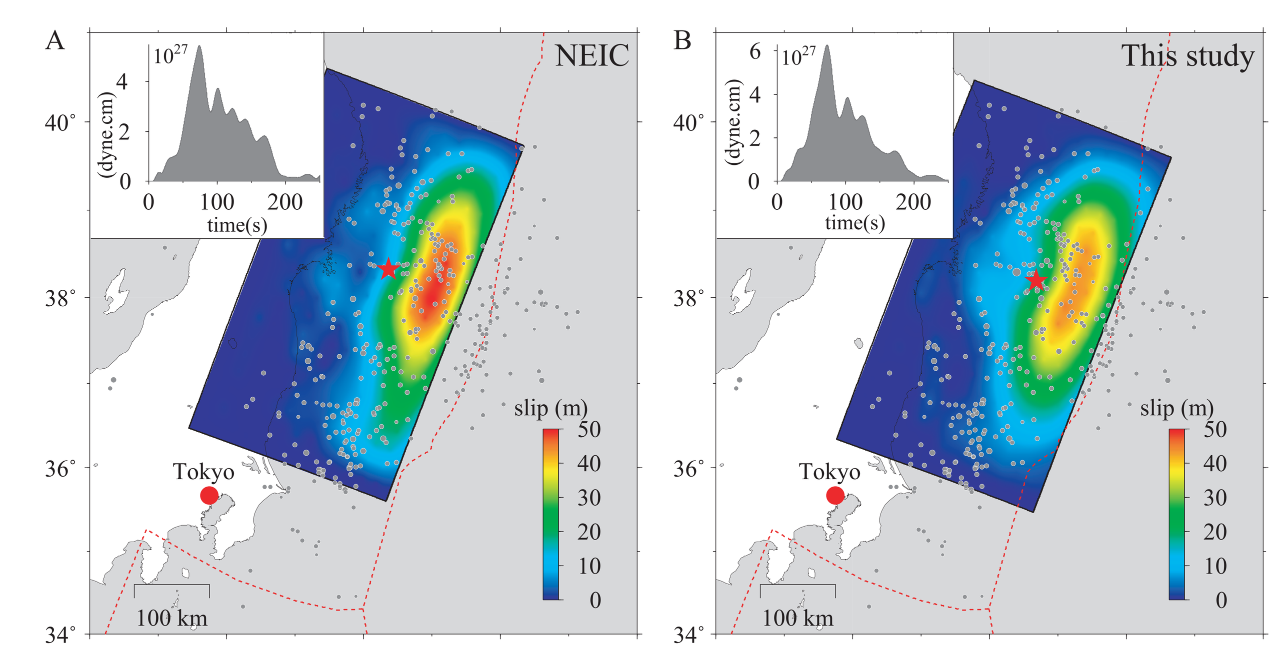

Figure 5. Sensitivity test on epicenter locations using composite finite-fault inversions of GPS and teleseismic P-waveform data. Map view of slip models are for (A) the refined epicenter location and (B) the NEIC location, respectively. Epicenter location is the only difference between the setup of these two inversions. Here, we use global CMT solution to define the dip (10°) and strike (203°) of the fault plane. Moment-rate plot is inserted to the upper left of each panel. Red stars indicate the epicenter locations and gray dots with white boundary are the aftershocks occurring in the first three days. Red dash lines denote plate boundaries (Bird, 2003). With the use of the refined hypocenter, not only is the entire pattern displaced as much as 20 km to the east but also some details of the slip and the moment rate function changed.

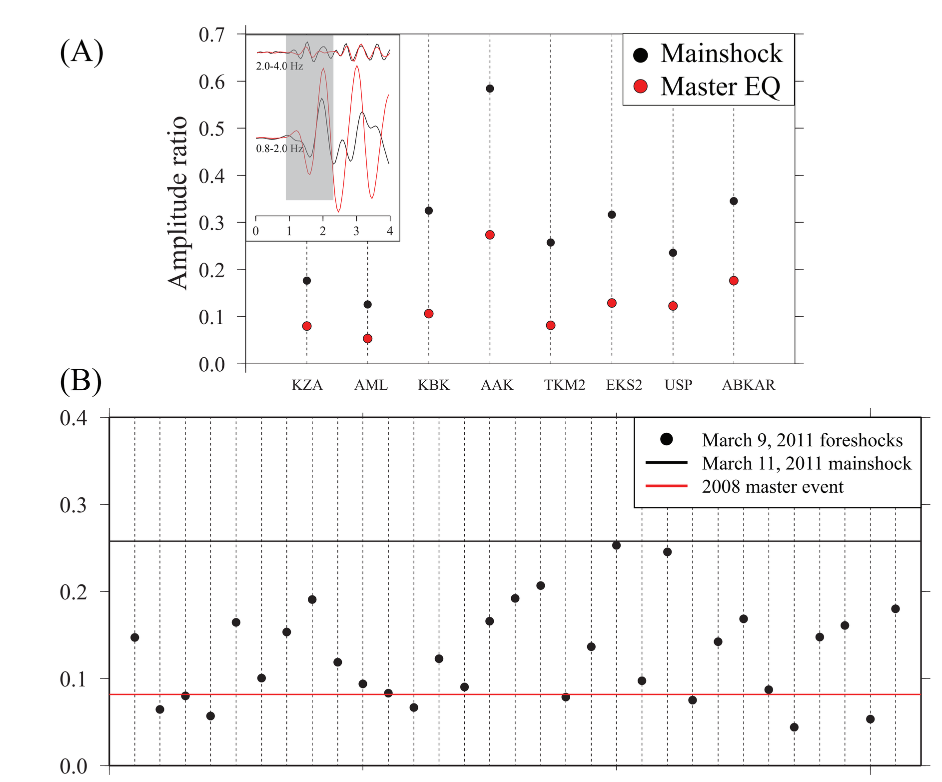

Figure 6. (A) High-frequency (2.0-4.0 Hz) amplitude and low-frequency (0.8-2.0 Hz) amplitude ratio for the master earthquake (red dots) and main-shock (black dots) at 8 stations (x-axis). The inset shows an example of time window for the measurements at station TKM2. (B) High-frequency/low-frequency amplitude ratio for station TKM2 for the 03/09/2011 foreshock sequence. Each dot represent an earthquake. The ratios for master earthquake and beginning of the mainshock are plotted as red line and black line, respectively. The 2011 Tohoku-Oki earthquake has relatively larger high-frequency energy than the 2008 earthquake and the 03/09/2011 foreshock sequences.